Clifford R. Jack, Jr, MD • Richard M. Thompson, MD • R. Kim Butts, PhD
Frank W. Sharbrough, MD • Patrick J. Kelly, MD • Dennis P. Hanson, BS
Stephen J. Riederer, PhD • Richard L. Ehman, MD • Nicholas J. Hangiandreou, PhD
Gregory D. Cascino, MD

Sensory Motor Cortex: Correlation of Presurgical Mapping with Functional MR Imaging and Invasive Cortical Mapping[1]

PURPOSE: **To describe a clinically useful application of functional magnetic resonance (MR) imaging—presurgical mapping of the sensory motor cortex—and to validate the results with established physiologic techniques.**

MATERIALS AND METHODS: **Functional MR mapping of the sensory motor cortex was performed in two women, aged 24 and 38 years. Both had intractable, simple partial motor seizures due to tumors located in or near the sensory motor cortex. They subsequently underwent invasive cortical mapping—direct cortical stimulation and/or sensory-evoked-potential recording—to localize the affected sensory motor area prior to tumor resection.**

RESULTS: **In both patients, the functional MR study demonstrated task activation of the sensory motor cortex. In both cases, results of cortical functional mapping with invasive techniques matched those obtained with functional MR imaging.**

CONCLUSION: **Presurgical mapping of the sensory motor cortex is a potentially useful clinical application of functional MR imaging.**

Index terms: Blood, flow dynamics • Brain, blood flow, 10.919 • Brain, function, 10.919 • Epilepsy • Magnetic resonance (MR), vascular studies

Radiology 1994; 190:85–92

If surgical resection of a lesion located in or near functionally essential cortex is considered, then localization of functional areas relative to the surgical target (the lesion) must be ascertained to avoid a postoperative neurologic deficit. This is particularly critical in patients whose only symptom is epilepsy. Such patients tend to have benign or indolent nonlife-threatening lesions, and a postoperative neurologic deficit may represent an unacceptable surgical risk. Traditionally, presurgical functional localization has been accomplished with invasive means: (*a*) direct cortical stimulation either intraoperatively in the awake patient or postoperatively after subdural grid placement or (*b*) sensory-evoked-potential studies after operative grid placement.

It has been shown recently that functional magnetic resonance (MR) imaging with blood oxygen level–dependent (BOLD) contrast is capable of noninvasively depicting primary sensory areas including the sensory motor cortex (1–9). However, studies to date have used volunteers and there has been no direct validation of the physiologic truth of functional localization with MR imaging. In this article we describe a clinically useful application of functional MR mapping of the sensory motor cortex for surgical planning. In addition, we compare the results of localization with functional MR imaging with the accepted criterion standard of invasive cortical mapping.

MATERIALS AND METHODS

Case 1

The patient was a 24-year-old woman who had been having simple partial motor seizures since she was 7½ years old. When she was evaluated at our institution, she was having two to five seizures per month despite treatment with an optimal antiepileptic medical regimen. Her seizures began with an aura of right facial numbness and a painful sensation in the throat followed by choking and speech arrest. Postictally she was dysarthric with a right facial droop. Seizures were not accompanied by loss of consciousness. At age 19 years, a computed tomography (CT) scan was reportedly negative, and at age 23 years an MR study demonstrated a left frontoparietal lesion (Fig 1). She was evaluated at our institution as a surgical candidate and was admitted for prolonged inpatient video-electroencephalographic monitoring with withdrawal of medication. Ictal onset was determined to be of left frontal origin. On the basis of both clinical and electroencephalographic criteria, the site of seizure onset was in or near the left sensory motor cortex. Preoperative testing also included speech, language, and neuropsychologic evaluation, the results of which were within normal limits. Physical examination revealed mild right facial weakness, but findings were otherwise negative. Cerebral angiography with amytal testing demonstrated left hemispheric speech dominance.

A functional MR examination with task activation of the sensorimotor cortex was performed with use of an approach similar to that described by Connelly et al (8). A series of short T1-weighted acquisitions in the axial and oblique planes were obtained to localize the tumor. From these T1-weighted images, several anatomic planes of interest were selected in which to perform functional MR imaging. The functional MR sequence consisted of obtaining 20 consecutive 3D SPGR images at a single section location with the following parameters: echo time, 60 msec; repetition time, 80 msec; flip angle, 40°; field of view, 24 cm; section thickness, 4 mm; one signal averaged; a 64 × 64 matrix; and 5.1 seconds per image. These images were obtained on a 1.5-T system (Signa; GE Medical Systems, Milwaukee, Wis) with standard hardware and software (the only software modification was that permitting use of the coarse acquisition matrix). During this 20-image acquisition, the patient

Abbreviations: BOLD = blood oxygen level dependent, 3D SPGR = three-dimensional spoiled gradient-recalled acquisition in the steady state.

[1] From the Departments of Diagnostic Radiology (C.R.J., R.M.T., R.K.B., S.J.R., R.L.E., N.J.H.), Neurology (F.W.S., G.D.C.), Neurosurgery (P.J.K.), and Biomedical Imaging Resource (D.P.H.), Mayo Clinic and Foundation, 200 First St SW, Rochester, MN 55905. Received June 2, 1993; revision requested July 27; revision received August 23; accepted September 7. Supported in part by Public Health Service grants no. R01 NS28374, R01 CA37993, and HL07269-15. **Address reprint requests to** C.R.J.

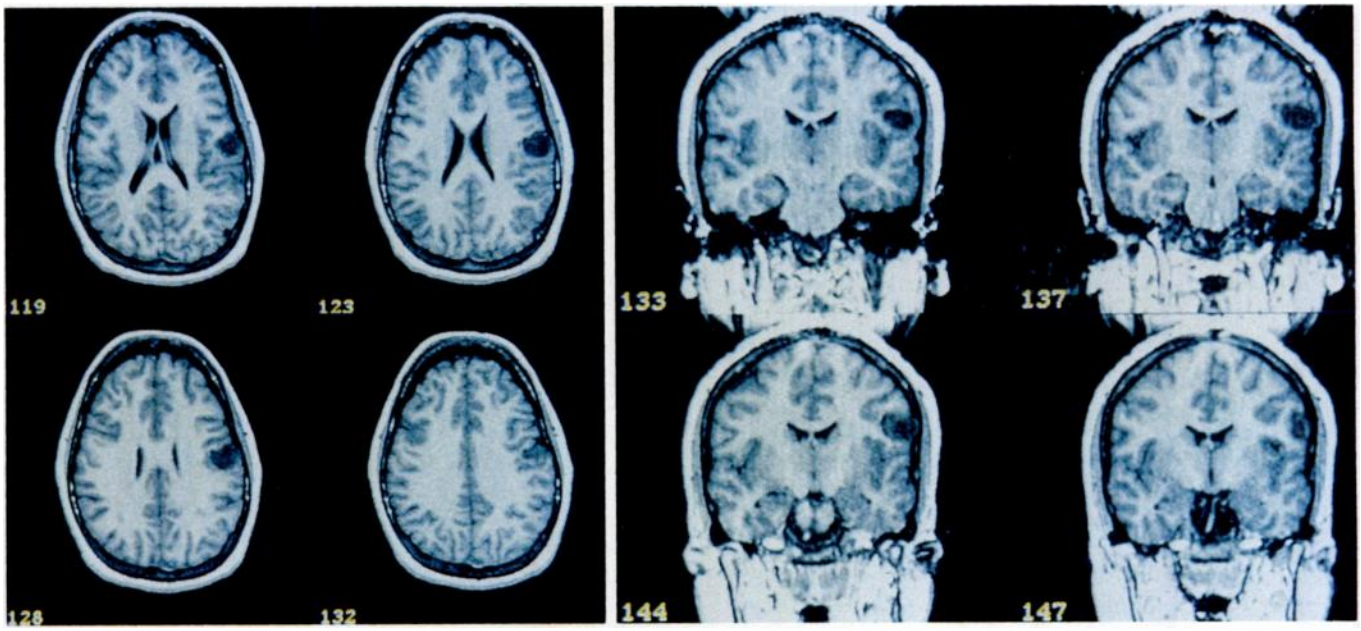

a. b.

Figure 1. Patient 1. Diagnostic MR images. **(a)** Axial and **(b)** reformatted coronal images from a three-dimensional spoiled gradient-recalled acquisition in the steady state (3D SPGR) sequence. These images demonstrate a peripherally located left frontoparietal tumor, with a complex relationship to the local normal sulcal anatomy. The inferior border of the tumor is at the brain surface and erodes the adjacent inner table, indicating its indolent nature.

alternated between rest and a voluntary activation task, which consisted of bilateral fingers to thumb opposition and contraction and relaxation of the lip and lower face muscles to activate the hand and lip–lower face portion of the sensory motor homunculus. The lip–lower face task was performed with no jaw motion (ie, only facial muscles around the mouth were moved) to minimize the possibility of head movement. Image processing consisted of simple image subtraction. The 20 images were partitioned into four clusters of five inactive, five active, five inactive, and five active images. The first image of each cluster was eliminated to produce a steady magnetization state for the first cluster of images and a physiologic steady state for the remaining three clusters. The active images were then added together and subtracted from the sum of the inactive images.

To anatomically link areas of activation on functional MR images to cortical surface anatomy, a volume rendering of the brain surface was performed with use of software (Analyze; Biomedical Imaging Resource, Mayo Clinic and Foundation, Rochester, Minn) (10). The brain was segmented from overlying structures by means of a series of mathematical erode, connect, and dilate morphology operations. The segmented MR imaging data were then loaded into a program that simultaneously displayed the volume-rendered image of the brain surface against the cross-sectional plane in which the functional MR images were obtained.

The patient subsequently underwent surgical implantation of a series of subdural recording strips. A small craniotomy was performed over the tumor, which had been localized stereotaxically. Three vertically oriented strips were placed above the tumor, and one horizontal T strip was placed below the tumor. Each recording strip consisted of eight circular stainless steel electrode contacts that were 4 mm in diameter, 10 mm in center-to-center distance, and embedded in a 75-mm-long Silastic (Dow Corning, Midland, Mich) sheath. Eight wire leads emerged from one end of the vertically placed strips and from the middle of the horizontally placed T strip. These leads passed through the craniotomy and were connected to the external circuitry. A cortical stimulation study was performed the following day. Current was passed between pairs of electrodes in a systematic fashion. The relationship between specific pairs of electrodes and elicited sensory and/or motor functions of the hand, foot, and face was recorded. Also recorded were those stimulation pairs that reproduced the patient's aura.

A thin-section CT study was then performed with the subdural recording strips in place. The CT study was co-registered with a 3D SPGR MR sequence obtained preoperatively by using a surface-matching algorithm (11). The position of each individual electrode contact was extracted from the registered CT data and was stored as a separate object in an object map. The brain and the tumor were segmented from the 3D SPGR images and were stored as separate objects in the object map. A volume-rendered image of the brain surface with the tumor and each individual electrode contact rendered as separate objects was generated by using a 24-bit color compositing multiple-object volume-rendering technique (10).

The patient then underwent surgical removal of the tumor. Prior to tumor removal, intraoperative sensory evoked potential tests were performed. Pathologic examination revealed a grade 2 oligodendroglioma. Postoperatively, findings at the patient's neurologic examination were unchanged.

Case 2

The second patient was a 38-year-old woman who was well until she experienced several secondarily generalized tonic-clonic seizures at age 30 years. MR imaging performed at that time demonstrated a right frontal intraaxial tumor (Fig 2). When she was seen at our institution, the patient was experiencing approximately two seizures per week despite receiving optimal medical therapy. These seizures began with an aura of numbness in the left hand or hemibody, and approximately 10% of the auras proceeded to become focal motor seizures involving the left upper and lower extremity with speech arrest but with no loss of consciousness. Preoperatively, single-section functional MR imaging was performed in several anatomic planes of interest. Separate hand and foot activation tasks were positioned as outlined for patient 1. Prolonged scalp-recorded inpatient video-electroencephalographic monitoring revealed right frontal seizure onset. During the surgical procedure, recording strips were placed over the paracentral cortex and sensory-evoked-potential tests with median nerve stimulation were performed to document the position of the central sulcus in relation to the tumor. The tumor

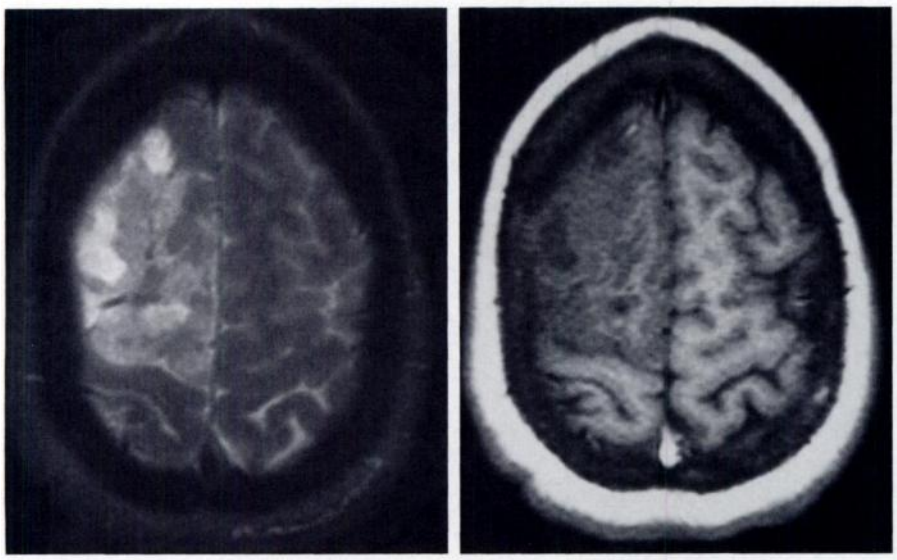

a. b.

Figure 2. Patient 2. Diagnostic MR images. Axial **(a)** T2-weighted and **(b)** T1-weighted images reveal an infiltrative right frontal tumor.

was removed and identified as a grade 3 oligodendroglioma. The patient experienced no motor deficit as a result of surgery.

RESULTS

Case 1

The functional MR images of this patient performing the task described demonstrated clear-cut cortical activation centered between two vertically oriented gyri. We expected these to be the pre- and postcentral gyri, with the activation centered in the central sulcus. On the basis of the findings in the functional MR study, we concluded that the tumor straddled the inferior portion of the central sulcus (Fig 3). The functional task administered should have activated both the hand and the lip–lower face portions of the sensorimotor homunculus (Fig 4) (12). In Figure 3b the majority of the activated area lies well above the tumor; the lowest portion of the activated strip is located at the uppermost border of the tumor. On the basis of findings in the images in Figure 3, we predicted that resection of the tumor would involve the lip–lower face portion of the sensorimotor homunculus but not the more cephalic hand area. As a rule, surgical damage to the hand or foot portion of the homunculus produces a severe functional deficit and is to be avoided, while damage to the face-lip portion will produce a clinically negligible deficit.

Figure 5 is a schematic drawing of the position of the four subdural recording strips in relation to the tumor and of the results of the cortical stimulation studies. Stimulation of the vertical strips revealed the expected orientation of the sensory motor homunculus of Penfield and Rasmussen (12). From the stimulation studies it was deduced that strip A was located over the motor cortex, strip B over the sensory cortex, and strip C posterior to the sensory cortex (Fig 5). The central sulcus was therefore located between strips A and B. Intraoperative sensory-evoked-potential recording with median nerve stimulation demonstrated maximum response at electrode 4 on strip B, thereby also confirming that strip B was over the primary sensory cortex. Stimulation between the lower electrodes on strips A and B, as well as between electrodes 4 and 5 on strip D, reproduced the patient's aura, a sensation in the throat. Intraoperatively, only the most inferior contacts of the three vertically oriented strips and contacts 4–6 of strip D were visible (Fig 6). The remaining contacts were hidden beneath the intact skull. Intraoperative photographs (Fig 6) document that the portion of the tumor at the brain surface was located between and inferior to contact 8 of strips A and B and above contacts 4 and 5 of strip D. Because of the limited exposure of the brain surface provided by the small craniotomy and because of the fact that the tumor had distorted normal local anatomic landmarks, an anatomic central sulcus could not be identified by inspecting the operative field. Because intraoperative inspection did not provide the desired correlation between the invasive stimulation studies and functional MR mapping, the following strategy was pursued.

A volume rendering of the brain surface was generated with the tumor and electrode contacts rendered as separate objects (Fig 7). This rendering demonstrated the relationship of individual electrode contacts to both the tumor and the cortical topography that could not be appreciated intraoperatively. This is a useful technique, because it enables correlation between the results of direct cortical stimulation and functional MR imaging. Visual comparison of the volume-rendered brain surface images in Figures 3 and 7 confirmed the impression formed from the functional MR study that the tumor straddled the functional sensorimotor strip.

Case 2

In patient 2, images of only one task (opposition of repetitive fingers to thumb) demonstrated convincing functional activation (Fig 8). Failed images were most likely a result of patient motion. As this patient had difficulty with head motion, the functional image (Fig 8) was generated with a single inactive-active cycle. Because of artifacts in this image, color mapping of functional activation onto a T1-weighted anatomic template was not effective. Instead, a linked-cursor display was used to identify common pixels in the T1-weighted and functional images (10). Figure 8b demonstrates a curvilinear area of activation centered on a sulcus (the central sulcus) that is posterior to the tumor. We inferred from this that the tumor extended posteriorly to but did not directly involve the primary motor strip. On the basis of findings in this image, we predicted that resection of the tumor would spare the primary motor cortex.

At surgery, the craniotomy was not extended beyond the posterior margin of the tumor, and therefore the relationship between the tumor and the cortical topography posterior to it could not be appreciated visually. However, intraoperative sensory-evoked-potential recording was performed by inserting subdural recording strips beneath the posterior margin of the craniotomy flap. Findings at left median nerve stimulation demonstrated that the central sulcus was located approximately 2 cm posterior to the posterior margin of the tumor, thus confirming the impression formed at functional MR imaging.

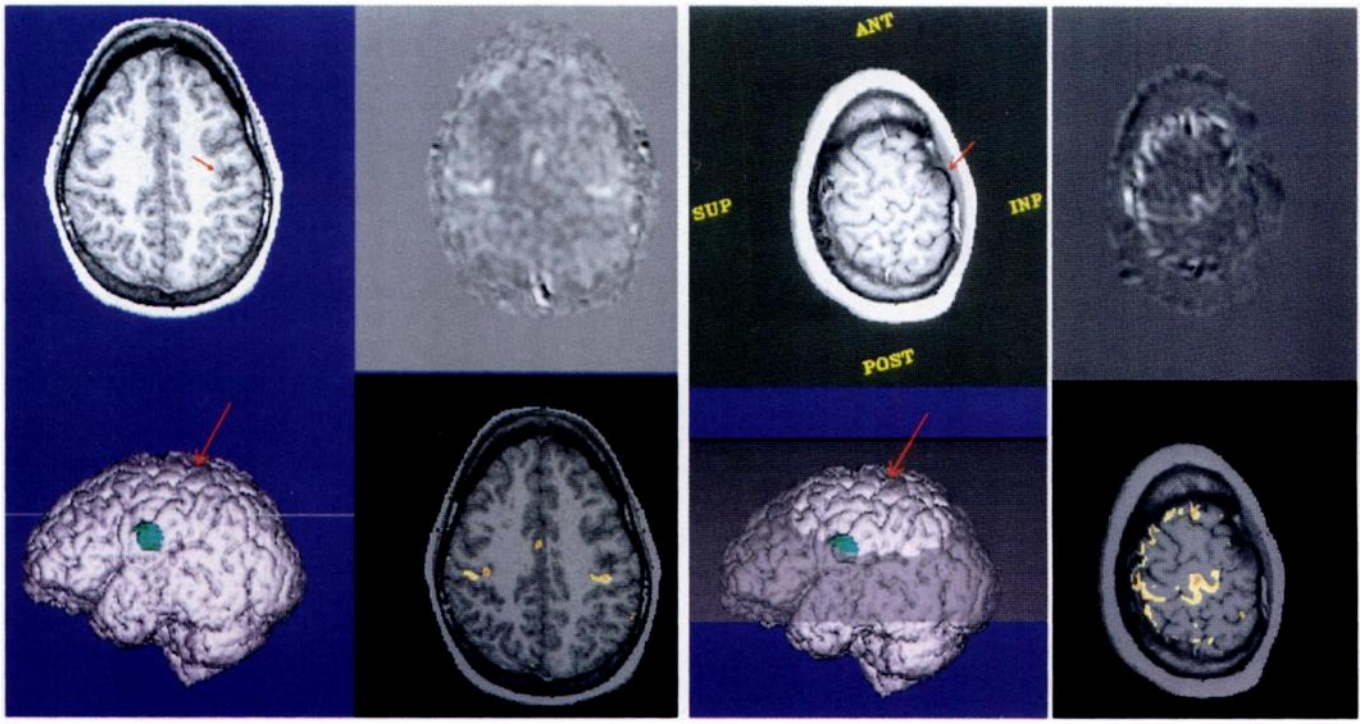

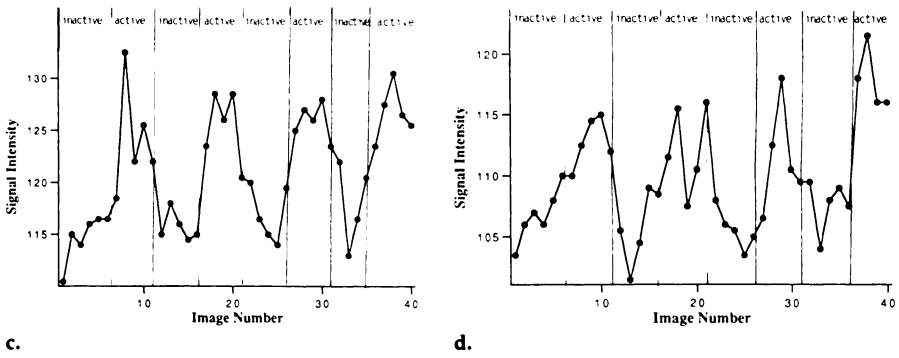

Figure 3. Patient 1. Functional MR images. **(a, b)** Four-panel collages. The upper left panel is a T1-weighted anatomic template of the cross section in which the corresponding functional MR imaging sequence was obtained (a small arrow indicates the position of the tumor). The upper right panel represents the functional activation image formed by the addition and subtraction process outlined herein. The lower right panel is created by assigning a color map to the functional image and then fusing that image with the T1-weighted anatomic template. The lower left panel represents a volume rendering of the brain surface with the tumor rendered as a separate green object and with the plane in which the functional MR image was obtained indicated by a line (as in **a**) or a shaded gray planar surface (as in **b**). Part **a** was obtained axially through the top of the tumor. Activation of the sensory motor cortex bilaterally is seen in the top right functional activation image. The relationship of the activated sensorimotor cortex in the patient's left hemisphere to the top of the tumor is illustrated in the fused image in the bottom right panel. Part **b** is an oblique section with anterior (*ANT*), posterior (*POST*), superior (*SUP*), and inferior (*INF*) labeled for orientation in the T1-weighted image in the top left panel. The curvilinear area of activation (top and lower right panels) precisely follows the contour of the central sulcus. The most inferior portion of this activated strip should represent the lip–lower face portion of the homunculus, whereas the more superior portion should represent the hand portion. The tumor is centered on and elevates the most inferior portion of the central sulcus, the top of which is indicated by a large arrow in the lower left images. **(c, d)** Time course plots of signal intensity in a manually defined region of interest. Part **c** is from a region of interest in the left sensorimotor area in **a**, and part **d** is from the sensorimotor area in **b**. Both **c** and **d** demonstrate a cyclic change in signal intensity, which follows the periodicity of the activation task.

DISCUSSION

Functional activation of the cortex with MR imaging was first demonstrated by means of a contrast bolus-tracking technique (13). It has been subsequently shown that this phenomenon can be visualized without exogenously administered contrast material (1–9). Fox and Raichle (14) demonstrated with positron emission tomography that appropriately designed stimulation paradigms will produce a local change in a number of physiologic parameters from baseline, in appropriate areas of the cortex. Most relevent to this type of imaging are the facts that cerebral perfusion will increase locally and will do so in excess of the oxygen metabolic rate. This results in both an increase in tissue perfusion and a paradoxical net decrease in concentration of deoxyhemoglobin in the capillary and venous bed of an activated area of cerebral cortex. Oxygenated hemoglobin is diamagnetic whereas deoxyhemoglobin is paramagnetic (15,16). The paramagnetic properties of deoxyhemoglobin create local field inhomogeneities, which decrease intravoxel spin coherence in the vicinity of blood vessels and thereby decrease the signal intensity on T2- or T2*-weighted MR images (15–20). Ogawa et al (17,18) suggested that the state of blood oxygenation may be a useful contrast parameter at MR imaging, and they coined the acronym BOLD contrast. Two possible mechanisms may contribute to the increased signal intensity seen in functionally activated cortical areas: One is the BOLD effect. The other is an increased flow of unsaturated spins into the imaging section which cycles in phase with the periodicity of the activation task. The precise interrelationship between these two mechanisms

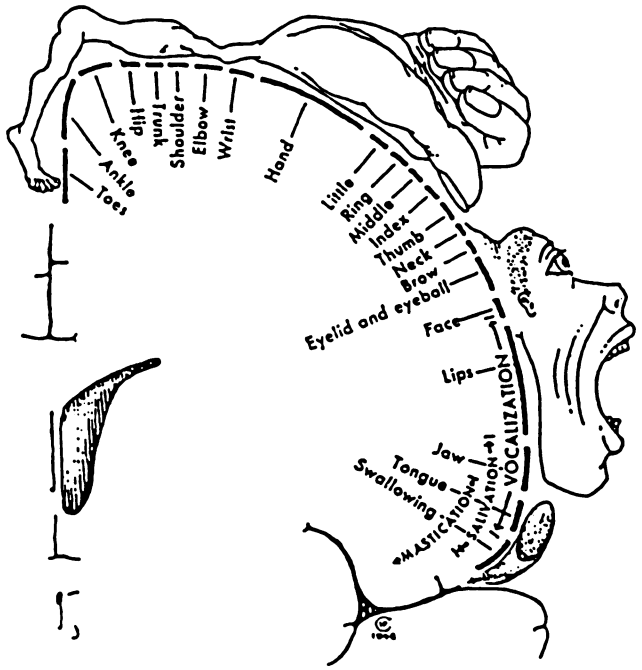

Figure 4. Motor homunculus. Pictorial representation of the location and relative extent of the different portions of the motor homunculus on the precentral gyrus. Analogous sensory areas are represented on the postcentral gyrus. (Reprinted, with permission, from reference 12.)

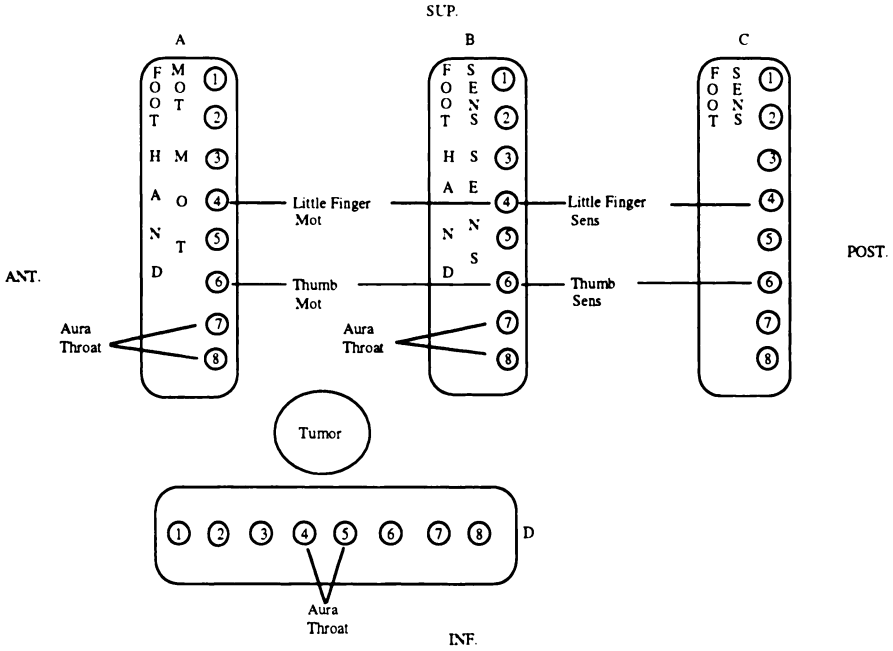

Figure 5. Patient 1. Subdural strips schematic of the position of the four subdural record strips (*A, B, C, D*) in relation to the tumor: anterior (*ANT*), superior (*SUP*), posterior (*POST*), and inferior (*INF*). *MOT* = motor response, *SENS* = sensory response. The central sulcus lies between strips in **a** and **b**. Results match the Penfield homunculus seen in Figure 4.

and observed activation-induced change in MR signal intensity is not yet clear. Use of a small flip angle and a phase-encoding scheme in which the central lines of K space are encoded first should decrease the effect of inflow enhancement; however, neither of these were employed in these two patients (5,7).

Most functional MR imaging work to date has focused on the BOLD effect. BOLD contrast results from a net decrease in concentration of deoxyhemoglobin in the capillary and venous system during task activation. Ideally, the accompanying changes in signal intensity at MR imaging serve as a precise marker of those areas of cortex that have undergone task activation. However, it is theoretically possible that the net influx of oxyhemoglobin into the venous system surrounding an area of activated cortex may be washed downstream, away from the specific area of task-activated cortex. Conceivably, alterations in signal intensity associated with task activation could be present in large superficial veins projecting over areas of cerebral cortex that were not involved in the activation process. If this were the case, then BOLD functional MR imaging would be far less specific and less useful for cortical mapping than if the alterations in signal intensity remained confined to the capillary bed or to small veins in the sulcus physically adjacent to the areas of cortex that were directly activated. It has recently been shown that the weighting of BOLD contrast with respect to vessel size varies as a function of both strength of static magnetic field and type of echo (20,21). Imaging at high field strength (4 T) and with a spin-echo technique produces greater contrast weighting for small vessels (ie, 3 μm or capillary level) than does imaging at lower field strength (1.5 T) or with a gradient-recalled echo. However, the observed activation-induced change in signal intensity is considerably smaller with spin-echo than with gradient-recalled-echo techniques. The inherently small contrast-to-noise ratio makes functional imaging with spin-echo techniques particularly challenging at 1.5 T. The implications for clinical applications of functional MR imaging are obvious. Few sites will ever have 4-T whole-body imagers. Therefore, clinical applications will likely be investigated at 1.5–2.0 T with use of techniques (ie, gradient echo) that favor visualization of veins rather than capillaries. This is a problem, however, only if the functional resolution of the MR technique is too coarse for the clinical task. In viewing the functional images of patient 1, particularly those in Figure 3b, it occurred to us that the activation signal intensity might partially or completely represent the large central sulcus vein seen on the patient's preoperative angiogram. However, when the morphology of the central sulcus vein (Fig 9) is compared with that of the activation signal intensity in Figure 3, a clear difference can be seen. We therefore conclude that while the activation signal intensity in Figure 3

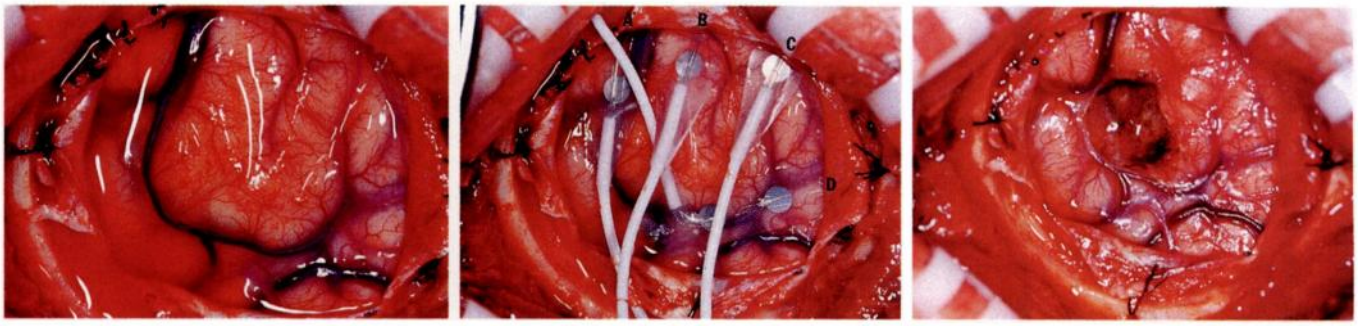

a. b. c.

Figure 6. Patient 1. Intraoperative photographs. After stereotaxic localization, a small burr hole was drilled directly over the tumor. **(a)** Cortical surface prior to placement of the recording strips and **(b)** strips on the cortical surface for comparison with Figure 5. The strips are labeled *A, B, C, D* as in Figure 5. Note only the most inferior electrode of the three vertical strips and electrodes 4, 5, and 6 of the horizontal strip are visible in the operative field, because the strips have been slipped beneath the dura beyond the craniotomy. For purposes of orientation, the patient's nose is on the reader's left, the top of the image is the superior part of the head, the electrodes in strip D overlie the sylvian fissure and the inferior part of the frontoparietal operculum. **(c)** The cortex after the tumor has been removed. The most inferior portion of the tumor was entered and the surgical plane extended superiorly beneath the brain surface. From this picture it is difficult to appreciate the entire extent of tumor removal, as the superior portion of the operative bed is concealed beneath undisturbed cerebral cortex. In comparison with Figure 9, note the tumor lies in the base of a U-shaped vein that extends in a cephalic direction, beneath the superior portion of the craniotomy flap.

may in part represent the effects of volume averaging of the superficially located central sulcus vein, it is more likely a result of signal in small veins in the deeper banks of the central sulcus that lie directly adjacent to the activated cortex.

The method employed here to generate functional MR images involved simple addition and subtraction of the time-course images. A drawback of this approach is that motion (brain or blood pulsation or bulk head motion) during data acquisition will tend to corrupt what is already a procedure with low signal-to-noise ratio. The rimlike high-intensity artifacts at the brain surface in Figures 3b and 8b demonstrate this problem. Pulsatile motion of cerebrospinal fluid—which is probably not a major problem in the images discussed herein because of the radio-frequency spoiling and large flip angle—will also corrupt functional images obtained with techniques that produce a high signal intensity in cerebrospinal fluid. Several attempts at producing functional MR images in patient 2 failed to show any obvious result, probably because of head motion during serial image acquisition. More sophisticated image processing procedures have been proposed such as *t* test or z maps designed to minimize these artifacts (22). A most promising approach by Bandettini et al (23) involves pixel-by-pixel thresholding according to the cross correlation between the shape of the time-course image data and that of the stimulus cycle.

Presurgical mapping of the sensorimotor cortex is an appealing clinical application of functional MR imaging. To our knowledge, results of functional MR studies published to date have not included rigorous physiologic correlation between presumed functional localization with functional MR imaging and actual localization with established invasive recording techniques. Surgery for epilepsy near functionally essential cortical areas is one of the few instances in which direct invasive brain mapping is indicated clinically, thus providing a unique opportunity for verifying the physiologic truth of functional MR imaging. Because this procedure is relatively uncommon (even in centers with a large volume of epilepsy surgery), experience with this correlation will accumulate slowly on a case-by-case basis. The two cases presented herein preliminarily support the fidelity of functional MR imaging in localizing the sensory motor cortex. The probable localization of the activation signal in small cortical veins (versus capillaries) does not appear to hamper this application significantly. Prior to widespread performance of functional MR imaging for this or other clinical uses, its accuracy must be validated against that of standard meth-

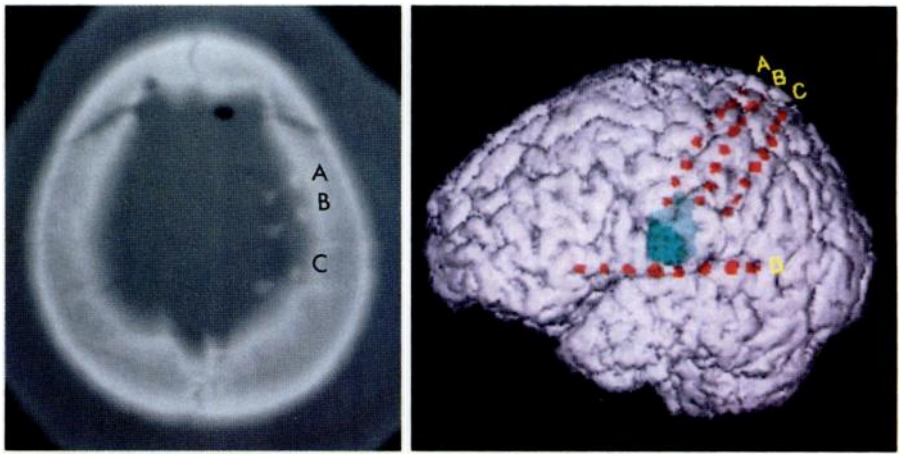

a. b.

Figure 7. Patient 1. **(a)** In CT scan with recording strips in place, the individual electrode contacts in strips *A, B,* and *C* can be seen over the left vertex. **(b)** Lateral view with the patient's head rotated slightly downward. The brain surface is rendered as a partially transparent object. The tumor is rendered in green, and that portion of the tumor that is at the brain surface appears brighter than the portion of the tumor that is deep to the brain surface. The eight individual electrode contacts of each of the four subdural strips are rendered as separate red objects. Strips *A, B, C,* and *D* are labeled as they are in Figure 5 and Figure 6. The central sulcus is shown by means of cortical stimulation to lie between strips *A* and *B*. Therefore, the tumor straddles the inferior portion of the central sulcus. Correlation of this image with that in Figure 3 confirmed the relationship between the localization of function on the cortical surface with functional MR imaging and that obtained with invasive recording.

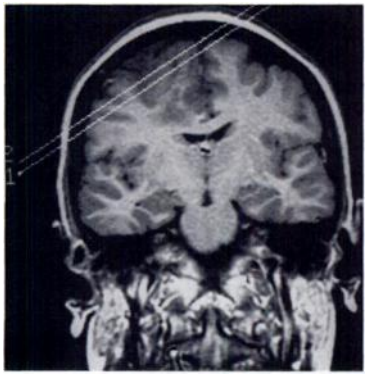

a.

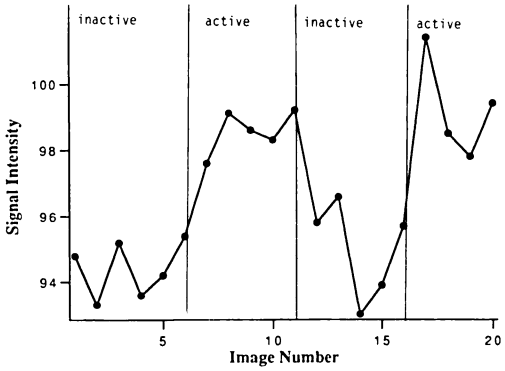

c.

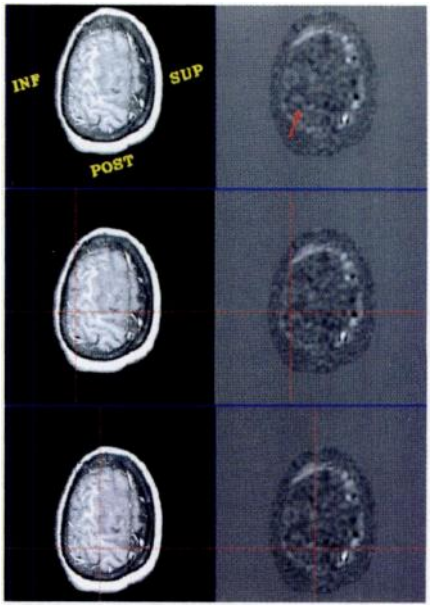

b.

Figure 8. Patient 2. Functional MR imaging study. **(a)** Coronal scout image with oblique axial planes cross referenced. **(b)** Images were obtained in section location 2. At top left is an obliquely oriented T1-weighted image through the tumor. Posterior (*POST*), superior (*SUP*), and inferior (*INF*) are indicated for orientation. Functional image at top right, obtained through the same section location as the T1-weighted map shows a hand movement activation task. A small S-shaped area of activation (arrow at top right) is seen in the posteroinferior aspect of the image, corresponding to hand activation. The middle and lower panel demonstrate a linked cursor display. The intersection of the cross hairs in the T1-weighted image corresponds to the same spatial coordinates in the adjacent functional image. These demonstrate that the S-shaped area of functional activation is centered on a sulcus (the central sulcus) that is located posterior and inferior to the tumor. On the basis of findings in the functional MR imaging study, we predicted that the primary motor cortex was located posterior to the tumor. **(c)** Time course plot of signal intensity in region of interest defined manually in the sensorimotor area in **b.** This was a single inactive-active cycle, as the patient had difficulty with head motion.

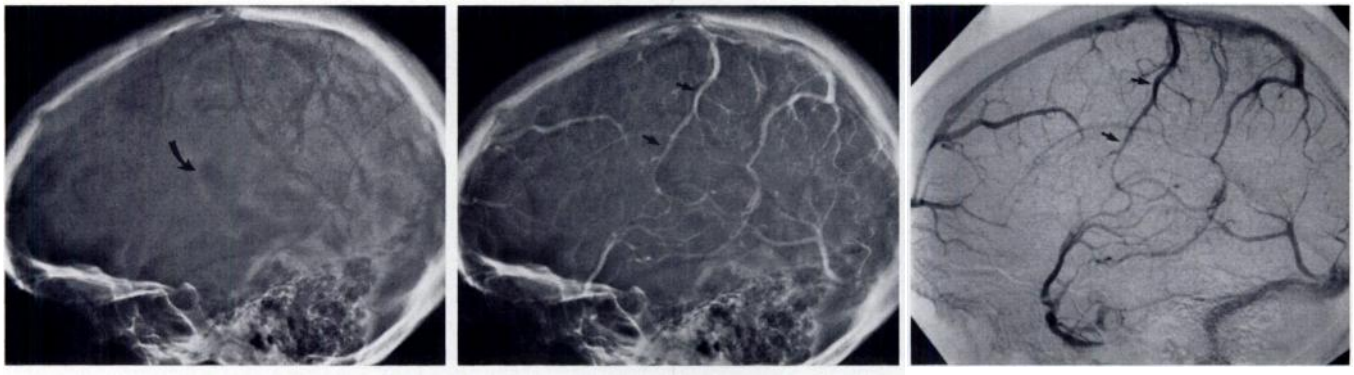

a. b. c.

Figure 9. Patient 1. Angiograms. **(a)** A lucent area (arrow) is seen in the midportion of the plain skull angiogram. **(b)** The venous phase of the angiogram demonstrates that this lucency is located precisely in the anteroinferior aspect of a U-shaped draining cortical vein (arrows). **(c)** A subtraction angiogram demonstrates the central cortical vein more clearly (arrows). Proof of the anatomic relationship between the tumor and this vein is obtained by comparing the shape of this vein in the angiogram with the shape of the draining vein that hugs the inferior aspect of the tumor in the intraoperative photographs of Figure 6. In turn, by comparing the shape of the vein with the curvilinear shape of the area of functional activation in Figure 3, one can see that although they are both located in the central sulcus, there is only a moderate physical correspondence between the two. The shape of the functional activation (Fig 3) is more complex and follows the curving contour of the portion of the central sulcus that lies deep to the surface. In contrast, the large central sulcus vein is less convoluted and lies on the brain surface.

ods of brain mapping. The cases reported herein illustrate a paradigm for performing these necessary validation studies. Because subdural recording grids or strips often lie partially under intact skull and may shift position during surgery, accurate intraoperative assessment of electrode position is difficult. Therefore, the functional-anatomic link between functional MR imaging and direct recording demonstrated in Figures 3 and 7 is particularly useful. ■

Acknowledgments: The authors thank Brenda Maxwell and Cindy Pfremmer of Mayo Biomedical Imaging Resource for manuscript typing.

References

1. Ogawa S, Tank DW, Menon R, et al. Intrinsic signal changes accompanying sensory stimulation: functional brain mapping with magnetic resonance imaging. Proc Natl Acad Sci USA 1992; 89:5951–5955.
2. Kwong KK, Belliveau JW, Chesler DA, et al. Dynamic magnetic resonance imaging of human brain activity during primary sensory stimulation. Proc Natl Acad Sci USA 1992; 89:5675–5679.
3. Bandettini PA, Wong EC, Hinks RS, et al. Time course EPI of human brain function during task activation. Magn Reson Med 1992; 25:390–397.
4. Turner R, Jezzard P, Wen H, Kwong KK, et al. Functional mapping of the human visual cortex at 4 and 1.5 Tesla using deoxygenation contrast EPI. Magn Reson Med 1993; 29:277–279.
5. Frahm J, Bruhn H, Merbloldt K, Hanicke W. Dynamic MR imaging of human brain oxygenation during rest and photic stimulation. JMRI 1992; 2:501–505.
6. Belliveau JW, Kwong KK, Kennedy DN, et al. Magnetic resonance imaging mapping of brain function: human visual cortex. Invest Radiol 1992; 27:S59–S65.
7. Menon RS, Ogawa S, Kim SG, et al. Functional brain mapping using magnetic resonance imaging: signal changes accompanying visual stimulation. Invest Radiol 1992; 27:S47–S53.

8. Connelly A, Jackson GD, Frackowiak RSJ, et al. High-resolution functional mapping of activated human primary cortex using a clinical magnetic resonance imaging system. Radiology 1993; 188:125–130.
9. Kim SG, Ashe J, Hendrich K, et al. Functional magnetic resonance imaging of motor cortex: hemispheric asymmetry and handedness. Science 1993; 261:615–617.
10. Robb RA. A software system for interactive and quantitative analysis of biomedical images. In: Höhne KH, Fuchs H, Pizer SM. 3D imaging in medicine. Springer-Verlag, Berlin, Germany: NATO ASI Series 1990; 60:333–361.
11. Jiang H, Robb RA, Holton KS. A new approach to 3-D registration of multimodality medical images by surface matching. SPIE 1992; 1808:196–213.
12. Penfield W, Rasmussen T. The cerebral cortex of man. New York, NY: MacMillan, 1950; 57.
13. Belliveau JW, Kennedy DN, McKinstry RC, et al. Functional mapping of the human visual cortex by magnetic resonance imaging. Science 1991; 254:716–719.
14. Fox PT, Raichle MR. Focal physiological uncoupling of cerebral blood flow and oxidative metabolism during somatosensory stimulation in human subjects. Proc Natl Acad Sci USA 1986; 83:1140–1144.
15. Brindle KM, Brown FF, Campbell ID, et al. Application of spin echo nuclear magnetic resonance to whole-cell systems. Biochem J 1979; 180:37–44.
16. Thulborn KR, Waterton JC, Matthews PM, et al. Oxygenation dependence of the transverse relaxation time of water protons in whole blood at high field. Biochim Biophys Acta 1982; 714:265–270.
17. Ogawa S, Lee TM, Kay AR, et al. Brain magnetic resonance imaging with contrast dependent on blood oxygenation. Proc Natl Acad Sci USA 1990; 87:9868–9872.
18. Ogawa S, Lee TM, Nayak AS, et al. Oxygenation-sensitive contrast in magnetic resonance image of rodent brain at high magnetic fields. Magn Reson Med 1990; 14:68–78.
19. Turner R, Le Bihan D, Moonen CTW, Despres D, Frank J. Echo-planar time course MRI of cat brain oxygenation changes. Magn Reson Med 1991; 22:159–166.
20. Ogawa S, Menon RS, Tank DW, et al. Functional brain mapping by blood oxygenation level-dependent contrast magnetic resonance imaging. Biophys J 1993; 64:803–812.
21. Weisskoff RM, Boxerman JL, Zvo CS, Rosen BR. Endogenous susceptibility contrast: principles of relationship between blood oxygenation and MR signal change. Presented at the Functional MRI of the Brain Workshop, Arlington, Va, June 17–19, 1993.
22. LeBihan D, Jezzood P, Turner R, Cuenode C, Zffiro T. Analysis of functional MR images with z maps: work in progress. JMRI 1993; 3(P):141.
23. Bandettini PA, Jesmanowicz A, Wong EC, Hyde JS. Processing strategies for time-course data sets in functional MRI of the brain. Magn Reson Med 1993; 30:161–173.